PAQR3 Modulates Insulin Signaling by Shunting Phosphoinositide 3-Kinase p110α to the Golgi Apparatus

Xiao Wang,[1] Lingdi Wang,[1] Lu Zhu,[1] Yi Pan,[1] Fei Xiao,[1] Weizhong Liu,[1] Zhenzhen Wang,[1] Feifan Guo,[1] Yong Liu,[1] Walter G. Thomas,[2] and Yan Chen[1]

Phosphoinositide 3-kinase (PI3K) mediates insulin actions by relaying signals from insulin receptors (IRs) to downstream targets. The p110α catalytic subunit of class IA PI3K is the primary insulin-responsive PI3K implicated in insulin signaling. We demonstrate here a new mode of spatial regulation for the p110α subunit of PI3K by PAQR3 that is exclusively localized in the Golgi apparatus. PAQR3 interacts with p110α, and the intracellular targeting of p110α to the Golgi apparatus is reduced by PAQR3 downregulation and increased by PAQR3 overexpression. Insulin-stimulated PI3K activity and phosphoinositide (3,4,5)-triphosphate production are enhanced by *Paqr3* deletion and reduced by PAQR3 overexpression in hepatocytes. Deletion of *Paqr3* enhances insulin-stimulated phosphorylation of AKT and glycogen synthase kinase 3β, but not phosphorylation of IR and IR substrate-1 (IRS-1), in hepatocytes, mouse liver, and skeletal muscle. Insulin-stimulated GLUT4 translocation to the plasma membrane and glucose uptake are enhanced by *Paqr3* ablation. Furthermore, PAQR3 interacts with the domain of p110α involved in its binding with p85, the regulatory subunit of PI3K. Overexpression of PAQR3 dose-dependently reduces the interaction of p85α with p110α. Thus, PAQR3 negatively regulates insulin signaling by shunting cytosolic p110α to the Golgi apparatus while competing with p85 subunit in forming a PI3K complex with p110α. ***Diabetes*** **62:444–456, 2013**

Insulin resistance is closely associated with the pathogenesis of metabolic diseases, especially type 2 diabetes (1). The phosphoinositide 3-kinase (PI3K)/AKT pathway is central to the metabolic actions of insulin (2,3), and the PI3K family is grouped into three classes (I–III) according to substrate preference and sequence homology. Class IA PI3K comprises heterodimers of a p85 regulatory subunit (p85α, p85β, and p55γ) and a p110 catalytic subunit (p110α, p110β, and p110δ). In response to stimulation by growth factors such as insulin, the p110 subunits catalyze the production of a lipid second messenger phosphatidylinositol-3,4,5-trisphosphate at the plasma membrane (PM). This second messenger, in turn, activates the serine/threonine kinase AKT and other downstream effectors (4,5). The catalytic subunits p110α and p110β are expressed ubiquitously, whereas p110δ is mainly localized in hematopoietic cells (2,3) and likely has actions related to immune cell development and activation (6,7). Mice deficient in either p110α or p110β display embryonic lethality (8,9), and p110α is considered the primary determinant of insulin signaling and insulin sensitivity in vivo. Mice heterozygous for a kinase-dead mutation in p110α have hyperinsulinemia, glucose intolerance, and increased obesity (10), whereas p110β does not contribute to insulin receptor substrate (IRS)–associated PI3K activity (10). Moreover, conditional deletion of p110α in the liver reduces insulin sensitivity and impairs glucose tolerance in the mouse (11), which is not rescued by overexpression of p110β. Finally, a pharmacological approach using a panel of inhibitors specific for different catalytic subunits of PI3K has indicated that p110α is the primary insulin-responsive PI3K required for insulin signaling (12). Interestingly, a role for p110β on insulin action and metabolic control remains unresolved, although it may act to aid in setting a phenotypic threshold for p110α activity (12). Selective deletion of p110β in the mouse liver leads to a certain degree of insulin resistance without affecting AKT phosphorylation, suggesting a kinase-independent mechanism of metabolic regulatory control (13).

PAQR3 belongs to the progesterone and AdipoQ receptor (PAQR) family in which AdipoR1 and AdipoR2 (i.e., PAQR1 and PAQR2) function as cell surface receptors for adiponectin, an adipocyte-secreted cytokine that regulates glucose and lipid metabolism (14,15). Although PAQR3 shares high sequence homology with AdipoR1/PAQR1 and AdipoR2/PAQR2 (16), it is not localized on the PM (17,18). Instead, PAQR3 is exclusively localized in the Golgi apparatus and was renamed RKTG (Raf kinase trapping to Golgi) due to its spatial regulation of Raf kinase (17). Subsequent characterization of PAQR3 indicates that it may function as a tumor suppressor by negatively regulating the Ras to ERK signaling cascade (19–21). Given that PAQR3 regulates Ras/ERK and G protein–coupled receptor signaling pathways by sequestering Raf kinase or Gβ subunit to the Golgi apparatus (17,22), we hypothesized that PAQR3 might also regulate insulin signaling in a spatial manner. As p110α is the primary molecule within the PI3K family that mediates insulin signaling and insulin sensitivity (10–12), we focused on the potential regulation of p110α by PAQR3. In this study, we provide in vitro and in vivo evidence for a unique role of PAQR3 in the spatial regulation of insulin signaling via a capacity to sequester the p110α subunit of PI3K to the Golgi apparatus, thereby limiting its activity.

RESEARCH DESIGN AND METHODS

Animal studies. All animals were maintained and used in accordance with the guidelines of the Institutional Animal Care and Use Committee of the Institute for Nutritional Sciences. All of the experimental procedures were carried out in

From the [1]Key Laboratory of Nutrition and Metabolism, Institute for Nutritional Sciences, Shanghai Institutes for Biological Sciences, Chinese Academy of Sciences, Graduate School of the Chinese Academy of Sciences, Shanghai, China; and the [2]School of Biomedical Sciences, The University of Queensland, Brisbane, Australia.

Corresponding author: Yan Chen, ychen3@sibs.ac.cn.

Received 27 February 2012 and accepted 1 August 2012.

DOI: 10.2337/db12-0244

This article contains Supplementary Data online at http://diabetes.diabetesjournals.org/lookup/suppl/doi:10.2337/db12-0244/-/DC1.

X.W. and L.W. contributed equally to this study.

accordance with the Chinese Academy of Sciences ethics commission with an approval number 2010-AN-8. *Paqr3*-null mice were generated as previously described, with deletion of the exon 2 whole (17,19). The *Paqr3*$^{-/-}$ mice were crossed with C57BL/6J for at least five generations. For studies of in vivo insulin signaling, male mice fed with normal chow at 8–10 weeks of age were fasted overnight, followed by intraperitoneal injection of insulin (5 units/kg body weight). The mice were killed after 5 min, and the liver and gastrocnemius muscle were excised and snap frozen for analyses.

Confocal microscopy and quantification of fluorescence signals. The confocal analyses with overexpression experiments were performed as previously reported (17,22). The Golgi localization was determined by immunostaining with antibodies against either Golgin-97 or GM130, two well-characterized Golgi markers. For the study of localization of endogenous p110α in HEK293T cells, the plasmid for PAQR3 short hairpin RNA (shRNA) or its control were transfected into cells, and the cells were fixed and stained with anti–human p110α and Golgin-97 antibodies. The fluorescence signals of endogenous p110α were mainly localized in three areas: the cytosol, Golgi apparatus, and nucleus (Fig. 2*A*). Assuming that nucleus-localized p110α is not able to participate in p110α-mediated signaling on the PM, we calculated the percentage of Golgi-localized p110α signal and cytosol-localized p110α signal, and the signals from both compartments add to 100%. The Golgi-localized p110α signal was obtained by direct measurement of the fluorescence signals delimited by Golgi marker Golgin-97 (and delimited by PAQR3 staining in the case of PAQR3 overexpression, as another Golgi marker could not be used due to limitation of secondary antibodies; in addition, PAQR3 itself is exclusively localized in the Golgi apparatus). The cytosol-localized p110α signals were obtained by subtracting the total fluorescence signals of a cell from the signals in the Golgi apparatus and the nucleus (delimited by Hoechst 33342 staining). The images presented in the figures were captured using standardized setting and exposure times. More than 100 cells were observed in three independent experiments, and at least 20 cells were randomly chosen and measured in each experiment group. For the assay using green fluorescent protein linked to the pleckstrin homology domain (GFP-PH) to analyze in vivo activation of PI3K, HepG2 cells were transfected with GFP-AKT2-PH together with a Myc-tagged PAQR3 or the pCS2+MT vector as control, followed by culture for 18 h and then stimulation with 100 nmol/L insulin for various times. The fluorescence intensity and the subcellular distribution of GFP-PH were quantified using LSM by Zeiss Confocal Microscopy Software. The integrated density of pixels was calculated for the whole cell and for the subregion of the PM compartment. The fluorescence signal in the PM compartment was calculated by subtracting the integrated density value of the subregion of PM from the value of the whole cell. The percentage of GFP-PH signal in PM was then divided by the integrated density value of the whole cell. Twenty cells were measured in each experimental group.

Fractionation of Golgi membranes from mouse liver. Golgi membranes were purified as described previously (23,24). In brief, mouse livers were homogenized in 0.5 mol/L sucrose in PM buffer (potassium phosphate, with pH at 6.7, and 5 mmol/L $MgCl_2$) with protease inhibitor cocktail (Thermo, Rockford, IL). The homogenate was layered on top of 0.86 mol/L sucrose, overlaid with 0.25 mol/L sucrose, and centrifuged for 60 min at 29,000 rpm in a rotor (SW-41; Beckman Coulter, Brea, CA). The 0.5 mol/L sucrose layer was collected (cytosol fraction). The interface between the 0.5 and 0.86 mol/L sucrose (intermediate fraction) was diluted to 0.25 mol/L sucrose and layered on top of 1.3 and 0.5 mol/L sucrose. After centrifugation for 30 min at 8,000 rpm in a rotor (SW-41), the enriched Golgi membranes were collected at the 0.5/1.3 mol/L sucrose interface. Equal amounts of protein of liver homogenate, cytosol, intermediate fraction, and Golgi membranes were used for immunoblotting.

Preparation of the cytosolic and membranous fractions. The cytosolic and membranous fractions were separated by using a Cell Fraction Kit (Biovision, Milpitas, CA). In brief, HEK293T cells were homogenized on ice, the homogenate was centrifuged for 10 min at 700*g* at 4°C, and the supernatant was a cytosol-containing fraction. The pellet was resuspended in Membrane Extraction Buffer Mix (Biovision), followed by centrifuging for 5 min at 1,000*g* at 4°C, and the membrane protein was collected in the supernatant. Equal amounts of cytosol or membrane protein were used for immunoblotting in the PAQR3 overexpression experiment, and 1.5-fold more membrane proteins than the cytosolic proteins were used in the PAQR3 knockdown experiment.

Measurement of PI3K activity and phosphoinositide (3,4,5)-triphosphate level. The primary hepatocytes from wild-type and *Paqr3*$^{-/-}$ mouse livers and HepG2 cells were treated with insulin (10 nmol/L for primary hepatocytes or 100 nmol/L for HepG2 cells) for various times, and then the cells were lysed for 20 min with 1 mL ice-cold lysis buffer (137 mmol/L NaCl, 20 mmol/L Tris-HCl at pH 7.4, 1 mmol/L $MgCl_2$, 1 mmol/L $CaCl_2$, 0.1 mmol/L sodium orthovanadate, 1% NP-40, and 1 mmol/L phenylmethylsulfonyl fluoride). The whole-cell lysate was incubated with antibodies against IRS-1 or phosphotyrosine overnight, followed by incubation with protein A/G-Sepharose for 2 h at 4°C, and washed with TNE buffer (10 mmol/L Tris-HCl at pH 7.4, 150 mmol/L NaCl, 5 mmol/L EDTA, and 0.1 mmol/L sodium orthovanadate). The PI3K activity was measured in immunoprecipitates with a PI3K ELISA kit (Echelon Biosciences, Salt Lake City, UT). Phosphoinositide (3,4,5)-triphosphate (PIP3) content in the cells was measured with a PIP3 ELISA kit, according to a protocol that was previously reported (25).

Immunohistochemistry for GLUT4. Skeletal muscle was fixed in 4% paraformaldehyde/PBS, frozen in OCT (Optimal Cutting Temperature; SAKURA, Torrance, CA), sectioned, and immunostained. Samples were permeabilized and blocked with 1% BSA, 3% normal goat serum, and 0.1% Triton X-100 in PBS, followed by antibody incubation and mounting. For quantitation of cell surface localization of GLUT4, Zeiss Confocal Microscopy Software was used to quantify total fluorescent values of GLUT4 and the signals localized at the cell surface. The percentage of GLUT4 signal at cell surfaces was divided by the total GLUT4 signal. Sections from three individual mice were quantified for each sample.

Glucose uptake. Mice were anesthetized after 6 h of fasting. Skeletal muscle was dissected and rinsed in Krebs-Henseleit bicarbonate (KHB) buffer supplemented with 0.1% BSA and followed by incubation in PBS or 100 nmol/L insulin for 15 min at 30°C. The tissues were then treated with 1 mmol/L 2-deoxyglucose (2DG) for 20 min. All KHB buffers were pregassed with 95% O_2-5% CO_2. Glucose uptake was stopped by washing the tissues in ice-cold PBS. Subsequent to assays, muscle strips were solubilized in 10 mM Tris-HCl, pH 8.0, followed by detection of the amount of 2DG using a 2DG Uptake Measurement Kit (Cosmo, Tokyo, Japan).

Statistical analysis. Student t test was used for most of the statistical analysis. Mann-Whitney U test was used for the Western blot data in which $n = 3$. A two-sided test was performed with all the analyses.

RESULTS

PAQR3 tethers PI3K p110α subunit to the Golgi apparatus. We first analyzed whether PAQR3 was able to tether the PI3K subunit to the Golgi apparatus. When p110α was overexpressed in HeLa cells, it was diffusely distributed in the cytosol (Fig. 1*A*). Intriguingly, when coexpressed with PAQR3, p110α was almost completely mobilized to the Golgi apparatus (Fig. 1*A*). On the other hand, overexpression of PAQR3 did not promote the Golgi localization of overexpressed p85α (Fig. 1*A*). In addition, overexpression of PAQR3 had no effect on the subcellular distribution of AKT and glycogen synthase kinase 3β (GSK3β) (Supplementary Fig. 1), two other major players involved in insulin signaling. Next, we used coimmunoprecipitation assays to determine whether PAQR3 can form a complex with p110α. When both PAQR3 and p110α were overexpressed, immunoprecipitation of p110α could pull down PAQR3 (Fig. 1*B*). Conversely, immunoprecipitation of PAQR3 could also pull down p110α (Fig. 1*C*). Furthermore, immunoprecipitation of endogenous PAQR3 with an anti-PAQR3 antibody could copurify endogenous p110α (Fig. 1*D*), further confirming an interaction between PAQR3 and p110α.

We next investigated the intracellular localization of endogenous p110α under the condition of PAQR3 knockdown (Fig. 2*A*). Previously, we identified a PAQR3 shRNA (no. 3–121) that has a high efficiency for knockdown of endogenous PAQR3 (Supplementary Fig. 2) (21). We found that knockdown by a specific PAQR3 shRNA could markedly reduce Golgi localization of endogenous p110α in comparison with a control shRNA (FG-12) (Fig. 2*A*). In FG-12–expressing cells, 27% of endogenous p110α was localized in the Golgi apparatus and 73% in the cytosol (Fig. 2*B*). However, the percentage Golgi localization of p110α was reduced to ~12% by PAQR3 knockdown (Fig. 2*B*). Concomitantly, endogenous p110α in the cytosol compartment was elevated to 88% from 73% by PAQR3 knockdown (Fig. 2*B*). These data, therefore, further corroborate the functional role of PAQR3 in altering the subcellular distribution of p110α.

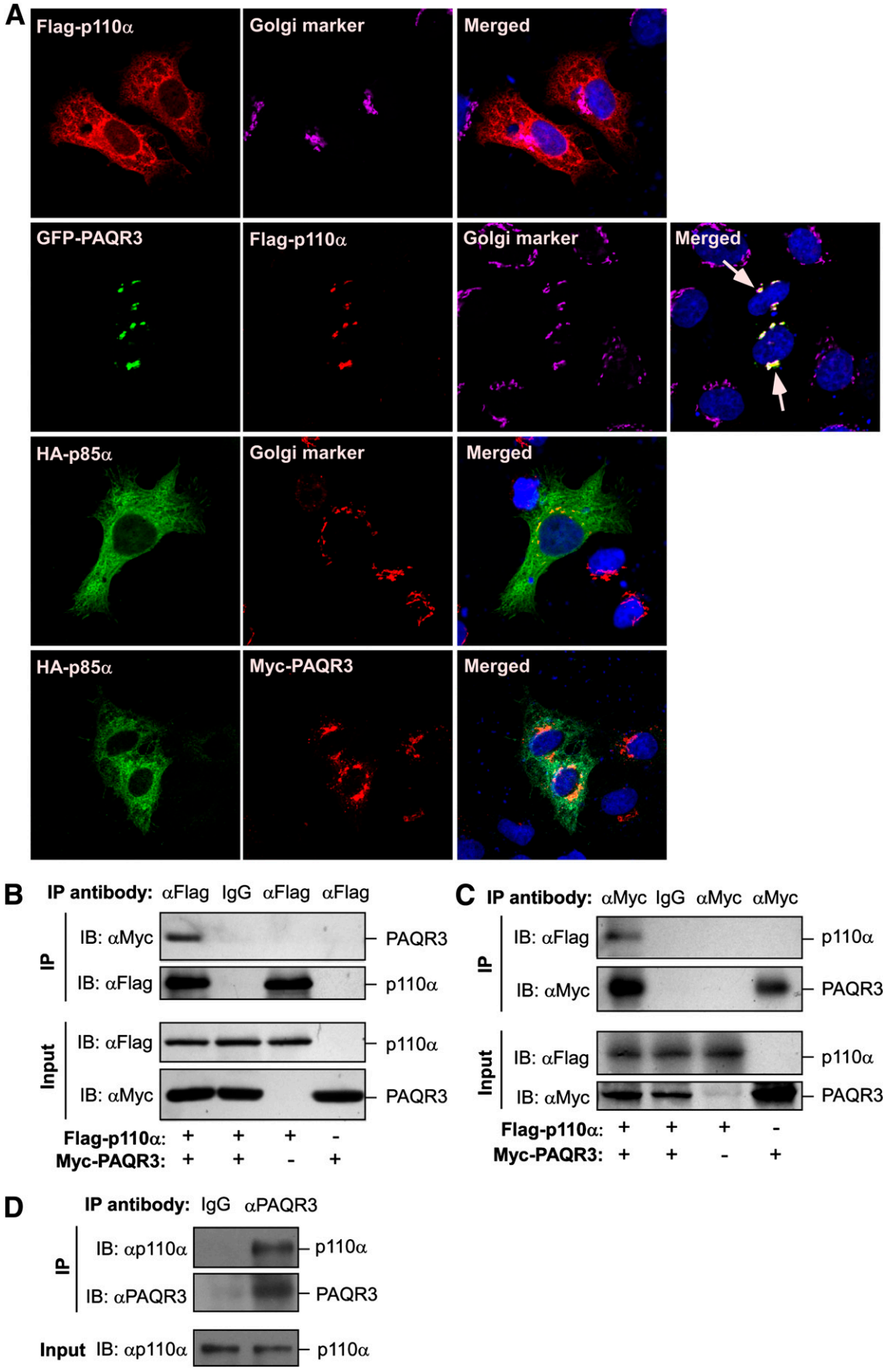

FIG. 1. PAQR3 tethers the p110α subunit to the Golgi apparatus and interacts with p110α. *A*: PAQR3 tethers overexpressed p110α, but not p85α, to the Golgi apparatus. HeLa cells were transiently transfected with the plasmids as indicated, followed by immunofluorescence staining and confocal

We also used a biochemical approach to purify Golgi complexes from mouse liver to assess the localization of endogenous p110α. In isolated liver from wild-type mice, p110α could be clearly detected in the Golgi fraction that coexisted with Golgi markers GM130 and Golgin-97 (Fig. 2*C*). However, ablation of PAQR3 led to marked reduction of Golgi compartmentalization of p110α in the liver (Fig. 2*C*), thus providing strong evidence that PAQR3 is implicated in Golgi localization of endogenous p110α protein.

Furthermore, we investigated the relative distribution of p110α in the cytosolic and membranous fractions. Silencing of PAQR3 expression caused a redistribution of p110α from the membranous fraction to the cytosol (Fig. 2*D*). Conversely, overexpression of PAQR3 reduced cytosolic distribution of p110α and increased membranous distribution of p110α (Fig. 2*E*). These data thus provide further evidence that PAQR3 can alter the subcellular compartmentalization of p110α.

PAQR3 is able to regulate PI3K activity. On the basis of our observations, we propose a model to illustrate the spatial regulation of PI3K by PAQR3 (Fig. 3*A*). We predict that PAQR3 negates insulin signaling by sequestering intracellular PI3K to the Golgi apparatus via the interaction with the p110α subunit. We next tested this model by directly analyzing the effect of PAQR3 on PI3K activity using two strategies. First, we measured the amount of PIP3, a direct product of PI3K. In primary mouse hepatocytes, as expected, insulin increased the level of PIP3 (Fig. 3*B*), which was further enhanced by ablation of *Paqr3* (Fig. 3*B*). Second, we analyzed PI3K activity using primary mouse hepatocytes. Insulin administration could rapidly stimulate PI3K activity, as assayed by immunoprecipitation of PI3K by antibodies against either IRS-1 or phosphorylated tyrosine (Fig. 3*C* and *D*). Deletion of *Paqr3* not only increased the basal PI3K activity but also enhanced insulin-stimulated PI3K activity (Fig. 3*C* and *D*). Conversely, overexpression of PAQR3 in HepG2 cells could significantly inhibit insulin-stimulated PIP3 production (Fig. 3*E*) and PI3K activity (Fig. 3*F*), corroborating the observations in *Paqr3*-deleted hepatocytes.

We also used an in vivo marker to directly analyze PI3K activation within the cell. A GFP fusion protein linked to the PH domain of AKT2 can be recruited to the PM upon insulin stimulation (26,27). Similar to the previous report (26), insulin treatment was able to rapidly elevate translocation of GFP-PH protein to the PM in HepG2 hepatocytes (Fig. 4). Interestingly, overexpression of PAQR3 markedly abrogated insulin-induced translocation of GFP-PH protein to the PM (Fig. 4). These data indicate that PAQR3 is directly involved in the functional regulation of PI3K, thus providing further evidence to corroborate the proposed model in which PI3K is modulated by PAQR3 in a spatial manner (Fig. 3*A*).

PAQR3 modulates insulin signaling in vitro and in vivo. We next analyzed the effect of PAQR3 on insulin signaling in hepatocytes. Insulin signaling is propagated by a series of protein phosphorylation events (28), initiated by insulin binding, activation, and phosphorylation of the insulin receptor (IR), and the subsequent phosphorylation of IRS, which functions as an adaptor for the p85/p110 PI3K complex. Activated PI3K generates PIP3, which recruits proteins, such as AKT, that contain specific lipid-binding domains (i.e., the PH domain). Activated AKT then phosphorylates a large array of proteins; one of the best characterized is GSK3. We analyzed the effect of PAQR3 on insulin-induced phosphorylation of four key proteins: IRβ (at Tyr1150/1151), IRS-1 (at Tyr608), AKT (at Ser473), and GSK3β (at Ser9). Insulin treatment induced rapid phosphorylation of IRβ, IRS-1, AKT, and GSK3β in hepatocytes (Fig. 5*A* and Supplementary Fig. 3), and the phosphorylation of AKT and GSK3β, but not IRβ and IRS-1, was markedly enhanced by *Paqr3* deletion (Fig. 5*A* and Supplementary Fig. 3). In contrast, overexpression of PAQR3 in HepG2 cells inhibited insulin-induced phosphorylation of AKT and GSK3β, but not IRβ and IRS-1, in HepG2 hepatocytes (Fig. 5*B* and Supplementary Fig. 4).

To investigate the in vivo role of PAQR3 on insulin signaling, we analyzed insulin signaling in the liver and skeletal muscle, two major insulin-responsive tissues. We administered insulin to wild-type and *Paqr3*-deleted ($Paqr3^{-/-}$) mice fed with normal chow. $Paqr3^{-/-}$ mice did not have any noticeable phenotype under normal resting conditions (17). As expected, insulin administration initiated rapid phosphorylation of IRβ, IRS-1, AKT, and GSK3β in mouse liver and skeletal muscle (Fig. 6*A* and *B*). Deletion of *Paqr3* had no effect on insulin-induced phosphorylation of IRβ and IRS-1, whereas insulin-stimulated phosphorylation of AKT and GSK3β was apparently enhanced by *Paqr3* ablation (Fig. 6*A* and *B*). The basal level of GSK3β phosphorylation was also elevated in the skeletal muscle of $Paqr3^{-/-}$ mice (Fig. 6*B*). Collectively, these data indicate that PAQR3 is able to modulate insulin signaling in vitro and in vivo. Furthermore, these findings demonstrate that PAQR3 exerts its effects on insulin signaling downstream of IRS but upstream of AKT, the place at which PI3K acts, consistent with our proposed model (Fig. 3*A*).

PAQR3 regulates insulin-induced glucose uptake in skeletal muscles. To further investigate the potential function of PAQR3 on insulin action, we analyzed whether PAQR3 could alter glucose uptake in skeletal muscles, one of the major physiological functions of insulin. We analyzed the translocation of GLUT4 of skeletal muscles upon insulin stimulation. As expected, insulin treatment could induce translocation of a portion of endogenous GLUT4 to the cell surface (Fig. 7*A*). Intriguingly, the insulin-induced translocation of GLUT4 to the PM was profoundly elevated by $Paqr3^{-/-}$ ablation (Fig. 7*A* and *B*). In addition, insulin-stimulated glucose uptake to the skeletal muscle was also enhanced by $Paqr3^{-/-}$ deletion (Fig. 7*C*). Collectively, these data reveal that PAQR3 not only alters insulin signaling but also affects the physiological actions of insulin.

PAQR3 prevents p85 subunit from forming a complex with p110α. We next analyzed the functional domains of PAQR3 and p110α that are involved in their interaction. Using a coimmunoprecipitation assay and various truncated versions of PAQR3 that we previously analyzed (17,18), we observed that the NH_2-terminal 71 amino acid residues of

analysis. The arrow indicates colocalization of p110α with PAQR3 at the Golgi apparatus. The Golgi apparatus was stained with either anti–Golgin-97 or anti-GM130 antibodies. The nuclei were stained with Hoechst 33342. *B* and *C*: Interaction of PAQR3 with p110α. HEK293T cells were transiently transfected with the plasmids as indicated. The cell lysate was used in immunoblotting (IB) and immunoprecipitation (IP) using the antibodies indicated. *D*: Interaction of endogenous PAQR3 with endogenous p110α. The cell lysate of HEK293T was used in IB and IP using the antibodies as indicated. (A high-quality digital representation of this figure is available in the online issue.)

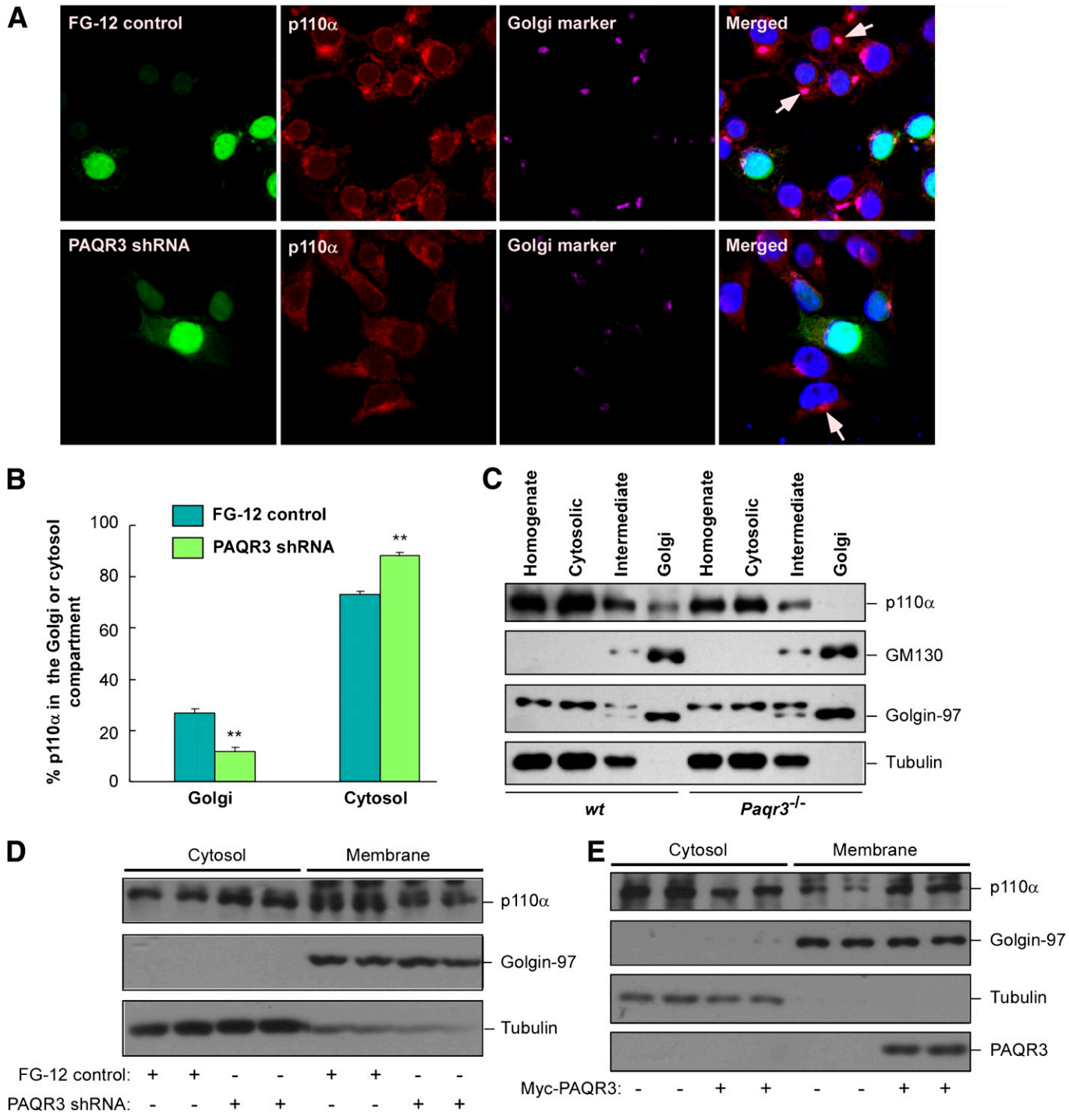

FIG. 2. Golgi localization of p110α is reduced by PAQR3 knockdown or deletion. *A* and *B*: Golgi localization of endogenous p110α is reduced by PAQR3 knockdown. HEK293T cells were transiently transfected with FG-12 control vector (*top*) or PAQR3 shRNA plasmid (*bottom*). Endogenous p110α was detected by an anti-human p110α antibody. The cells were examined through immunofluorescence staining and confocal analysis. The arrow marks the apparent Golgi localization of endogenous p110α in untransfected and FG-12–transfected cells. The percentage of endogenous p110α fluorescence signals in both the Golgi and cytosol compartments were calculated and shown as means ± SEM (*B*). ***P* < 0.01, PAQR3-shRNA group vs. the FG-12 control. The same experiment was performed more than three times with similar results. *C*: *Paqr3* ablation reduces Golgi localization of p110α. Golgi fractionation was performed with livers isolated from *Paqr3*-deleted mice and their littermate controls. Equal amounts of protein of liver homogenate, cytosol fraction, intermediate fraction, and Golgi membranes were used in immunoblotting with the antibodies, as indicated. *D* and *E*: PAQR3 alters the distribution of p110α in cytosolic and membranous fractions. The cytosolic and membranous fractions were separated from HEK293T cells in which PAQR3 was either silenced (*D*) or overexpressed (*E*). The proteins of each fraction were used in immunoblotting with the antibodies as indicated. This experiment was repeated three times with similar results. (A high-quality digital representation of this figure is available in the online issue.)

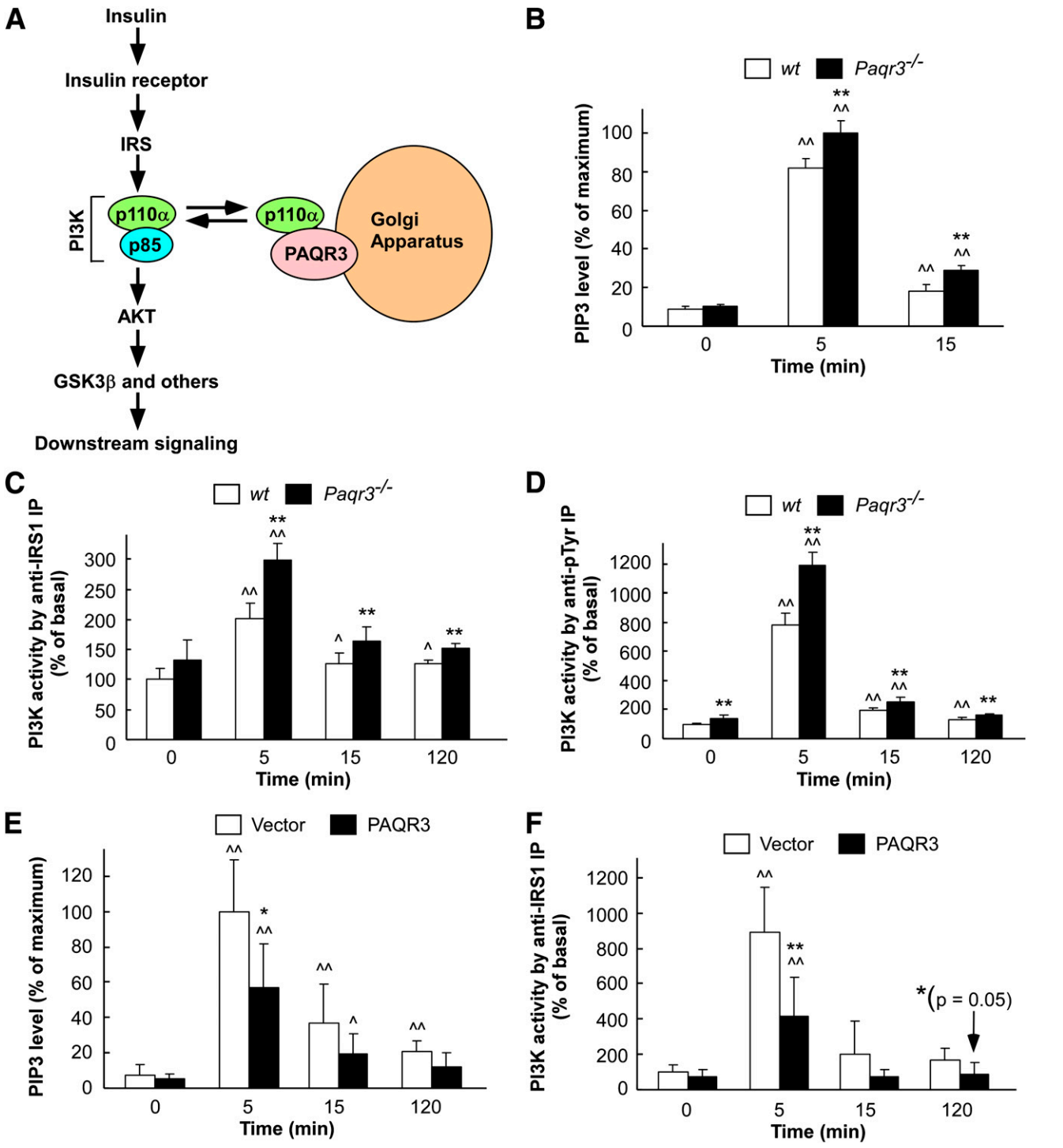

FIG. 3. PAQR3 is directly involved in the regulation of PI3K activity. *A*: A model of PAQR3 regulation on insulin signaling through shunting p110α to the Golgi apparatus. *B–D*: Insulin-stimulated PIP3 production and PI3K activity are increased by *Paqr3* ablation in mouse hepatocytes. Primary hepatocytes isolated from *Paqr3*-ablated mice and their littermate controls were treated with insulin for the times indicated, followed by measurement of the PIP3 level (*B*) and PI3K enzyme activity (*C* and *D*). Data are shown as mean ± SD ($n = 3$ for each group). **$P < 0.01$ between wild-type and *Paqr3*$^{-/-}$ cells at each time point. ^$P < 0.05$ and ^^$P < 0.01$ between insulin-treated and insulin-untreated cells with the same genotype. *E* and *F*: Insulin-stimulated PIP3 production and PI3K activity are inhibited by PAQR3 overexpression. HepG2 cells, transfected with PAQR3-expressing plasmid or the vector control, were treated with insulin for the length of time as indicated, followed by measurement of the PIP3 level (*E*) and PI3K enzyme activity (*F*). The data are shown as mean ± SD. *$P < 0.05$ and **$P < 0.01$ between control and PAQR3-overexpressing cells at each time point. ^$P < 0.05$ and ^^$P < 0.01$ between insulin-treated and insulin-untreated cells with the same transfection. (A high-quality color representation of this figure is available in the online issue.)

PAQR3 (PAQR3-N71) were sufficient to mediate the interaction with p110α (Fig. 8*A*). Further deletion of the NH_2 terminus of PAQR3 abrogated its interaction with p110α (Fig. 8*A*). In addition, PAQR3-N71 was able to inhibit insulin-stimulated AKT phosphorylation, similar to the effect of full-length PAQR3 (Supplementary Fig. 5), indicating that the NH_2 terminus of PAQR3 is sufficient to mediate the inhibitory effect of PAQR3 on insulin signaling.

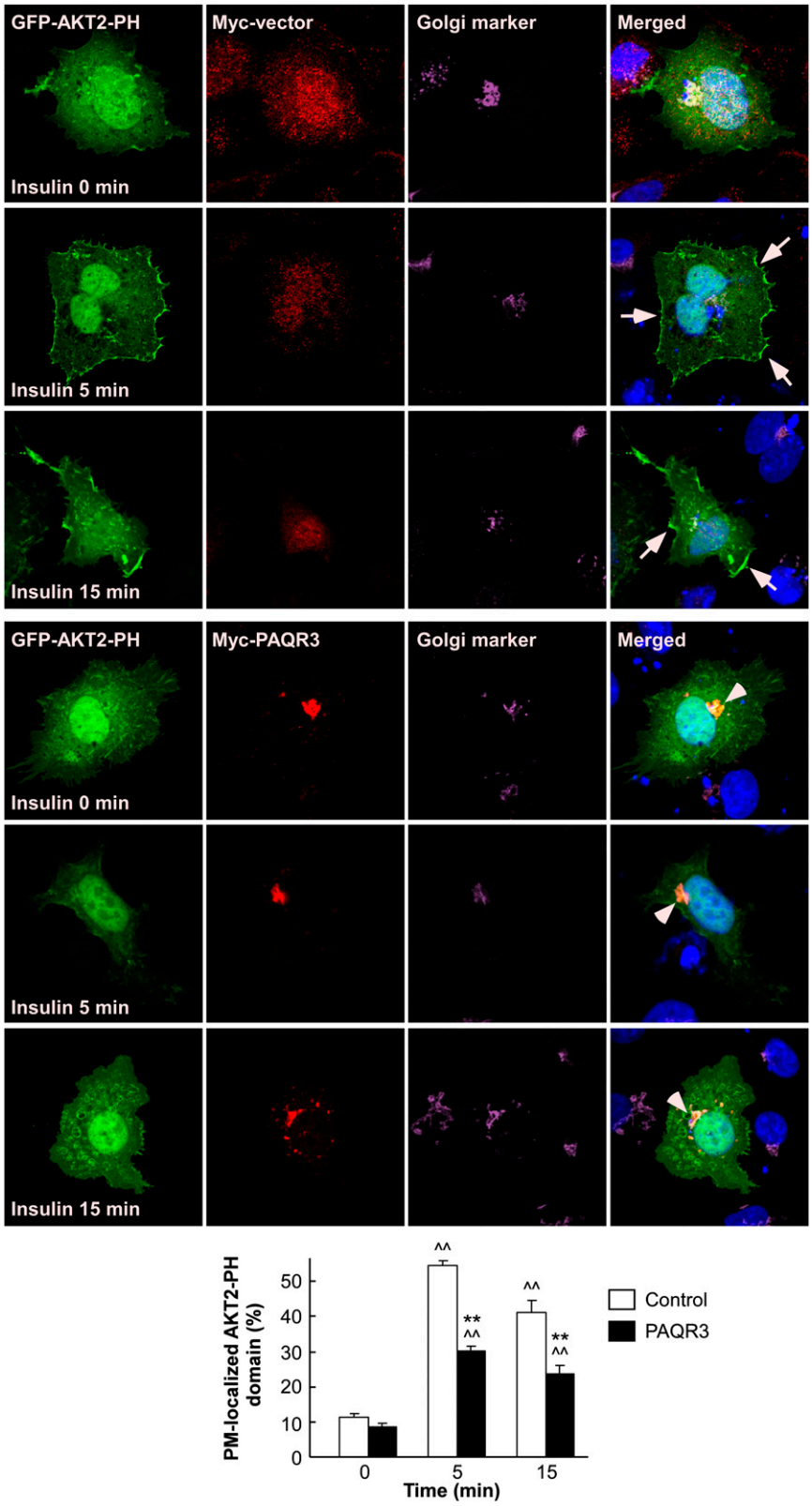

FIG. 4. In vivo PI3K activity is modulated by PAQR3. HepG2 cells were transfected with a Myc vector or Myc-tagged PAQR3 together with a GFP-fused PH domain of AKT2 that reports on in vivo activation of PI3K. The cells were treated with insulin for different lengths of time and then used in immunostaining and confocal analysis. Note that insulin treatment initiated clear enrichment of GFP-PH on the PM in control cells (arrow) but not in PAQR3-overexpressing cells in which PAQR3 was localized in the Golgi apparatus (arrowhead). The relative fluorescence intensity of GFP-PH on the PM was shown in the bottom panel as means ± SEM. **$P < 0.01$ between the control and PAQR-overexpression groups at each time point. ^^$P < 0.01$ between insulin-treated and insulin-untreated conditions within the same group. (A high-quality digital representation of this figure is available in the online issue.)

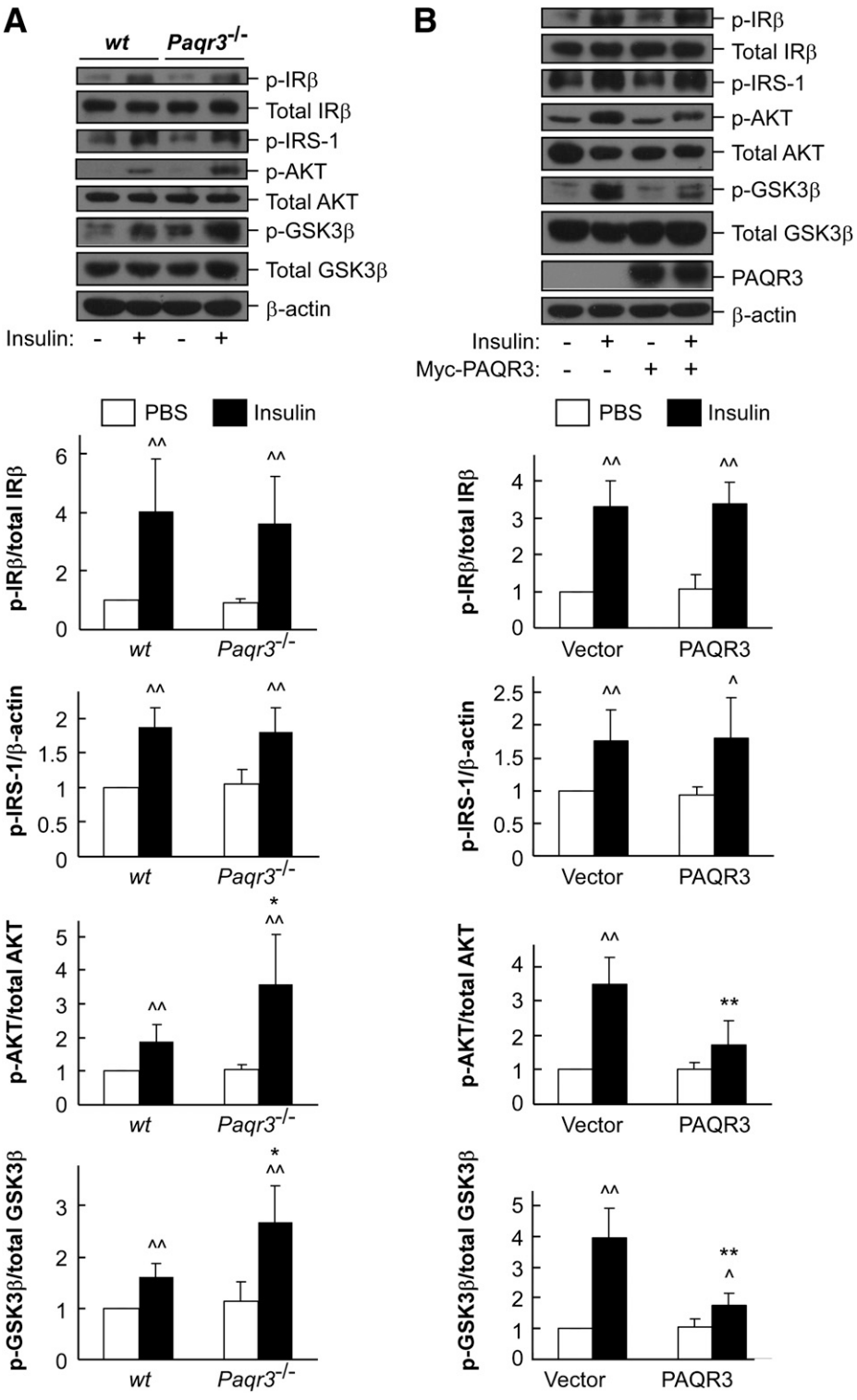

FIG. 5. Insulin signaling is altered by the expression level of PAQR3. *A*: Insulin signaling is enhanced by *Paqr3* deletion in hepatocytes. Primary hepatocytes were isolated from *Paqr3*-deleted mice and their littermate controls. The cells were treated with insulin (10 nmol/L) for 15 min, followed by immunoblotting with antibody as indicated. Five independent experiments were performed and gave rise to similar results. *B*: Overexpression of PAQR3 reduces insulin signaling. HepG2 cells were transiently transfected with a Myc-tagged PAQR3 plasmid as indicated, treated with insulin (100 nmol/L) for 15 min, and followed by immunoblotting. The expression of transfected PAQR3 was detected by an anti-Myc antibody. For both *A* and *B*, five independent experiments were performed and gave rise to similar results. The relative ratios of phosphorylated IRβ vs. total IRβ, phosphorylated IRS-1 vs. β-actin, phosphorylated AKT vs. total AKT, and phosphorylated GSK3β vs. total GSK3β were obtained by densitometric analysis, with the data shown under the immunoblots (mean ± SD). *$P < 0.05$ and **$P < 0.01$ between wild type (wt) and $Paqr3^{-/-}$ or between vector and PAQR3-overexpression groups with the same treatment. ^$P < 0.05$ and ^^$P < 0.01$ between saline- and insulin-stimulated cells.

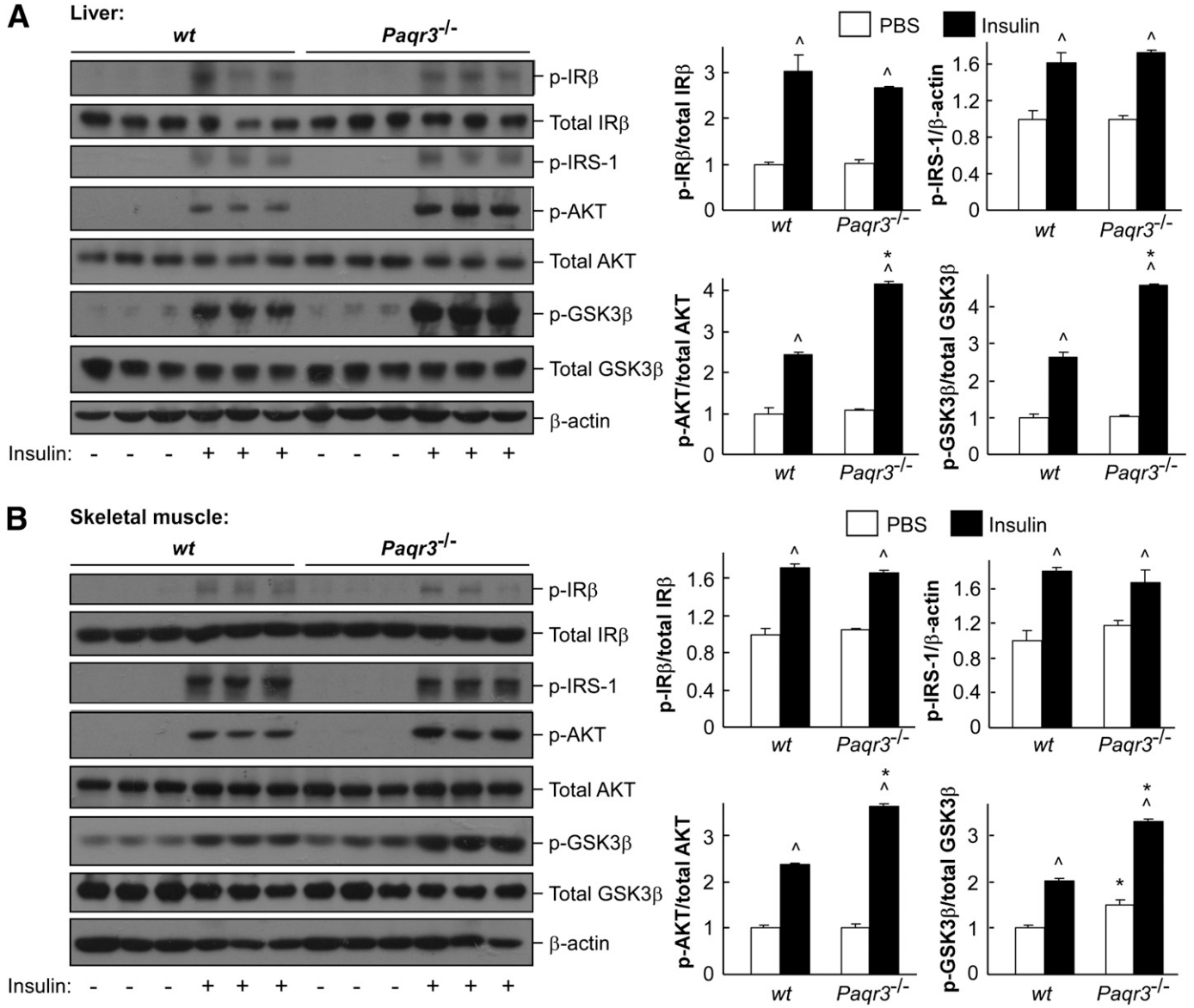

FIG. 6. Insulin signaling is enhanced by *Paqr3* deletion in mouse tissues. Insulin-stimulated phosphorylation of AKT and GSK3β, but not of IRβ and IRS-1, is enhanced by *Paqr3* deletion in the liver (*A*) and skeletal muscle (*B*). *Paqr3*-deficient mice and the littermate controls (at 8–10 weeks of age) fed with normal chow were fasted for 12 h, followed by intraperitoneal injection of saline or insulin. The animals were killed at 5 min after injection, and the livers and skeletal muscle were used in immunoblotting with the antibodies as indicated. The experiments were repeated at least three times for each tissue with similar results. The relative ratios of phosphorylated IRβ vs. total IRβ, phosphorylated IRS-1 vs. actin, phosphorylated AKT vs. total AKT, and phosphorylated GSK3β vs. total GSK3β were obtained by density analysis with the data shown in the right panels (means ± SEM). *P = 0.10 between wild-type (wt) and *Paqr3*$^{-/-}$ groups with the same treatment. ^P = 0.10 between saline- and insulin-injected mice with the same genotype. Two-sided Mann-Whitney U test was used in the statistical analysis.

We next used PAQR3-N71 to map the domain of p110α implicated in its interaction with PAQR3. Intriguingly, the p85 binding domain of p110α was sufficient to mediate the interaction with PAQR3 (Fig. 8*B*). On the basis of this finding, we hypothesized that PAQR3 might negate PI3K activity by reducing complex formation between the p85 subunit and p110α. To test this hypothesis, we analyzed the effect of PAQR3 on the p110α-p85α interaction. When PAQR3 was overexpressed, it could dose-dependently reduce the interaction of p110α with p85α (Fig. 8*C*). These data, therefore, indicate that PAQR3 negatively modulates PI3K activity by preventing the p85 subunit from binding to p110α while sequestering p110α to the Golgi apparatus.

PAQR3 expression is altered in insulin-resistant conditions, and *Paqr3* ablation increases insulin sensitivity. We next investigated the expression level of PAQR3 in obese and insulin-resistant mice either induced by high-fat diet (HFD) or caused by genetic deletion of leptin (*ob/ob* mice). The mRNA level of PAQR3 was elevated in the livers of both HFD and *ob/ob* mice (Fig. 9*A* and *B*). In addition, the mRNA level of PAQR3 was increased in glucosamine-induced insulin-resistant hepatocytes (Fig. 9*C*). These data, therefore, indicate that the expression level of PAQR3 is associated with the development of insulin resistance.

We also analyzed whether PAQR3 is implicated in the modulation of insulin sensitivity in vivo. The body weight

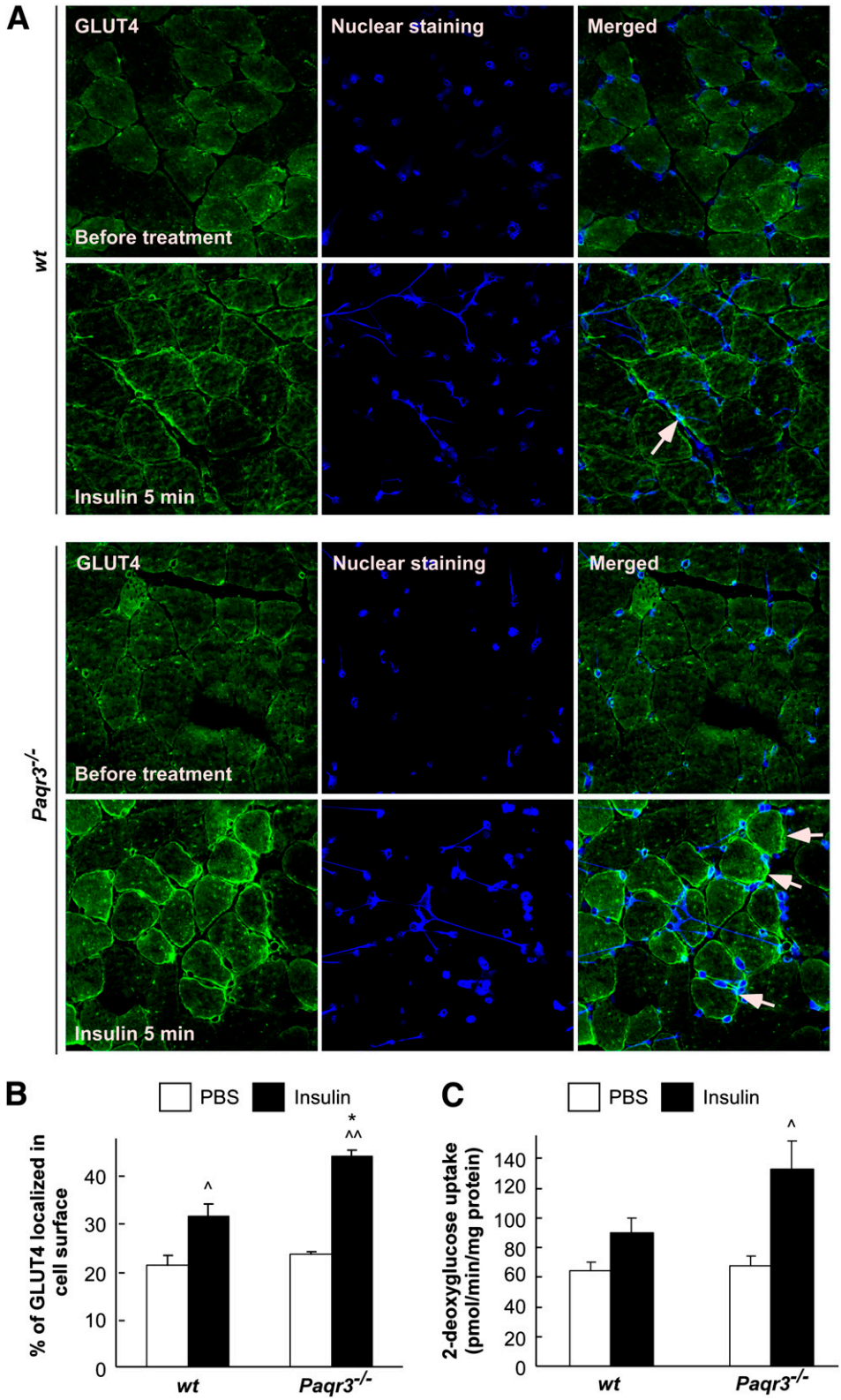

FIG. 7. Insulin-stimulated GLUT4 translocation to PMs and glucose uptake are increased by *Paqr3* ablation. *A* and *B*: GLUT4 translocation to the cell surface is modulated by PAQR3. Skeletal muscle from wild-type (wt) or *Paqr3*$^{-/-}$ mice that had been injected with either PBS or insulin was sectioned and stained with antibody for GLUT4. The sections were counterstained with Hoechest 33342. Original magnification ×40. The arrow indicates apparent translocation of GLUT4 to the cell surface. The percentage of GLUT4 in the cell surface is shown in B. *C*: Glucose uptake is regulated by PAQR3. Strips of skeletal muscle isolated from wt or *Paqr3*$^{-/-}$ mice were incubated in the absence (before treatment) or presence of 100 nM insulin prior to incubation in the presence of 1 mmol/L 2DG, followed by measurement of 2DG uptake. Six mice per group were used for the assay. For both *B* and *C*, the data are presented as mean ± SEM. **P* < 0.05 between wt and *Paqr3*$^{-/-}$ groups with the same treatment. ^*P* < 0.05 and ^^*P* < 0.01 between PBS- and insulin-treated mice with the same genotype. (A high-quality digital representation of this figure is available in the online issue.)

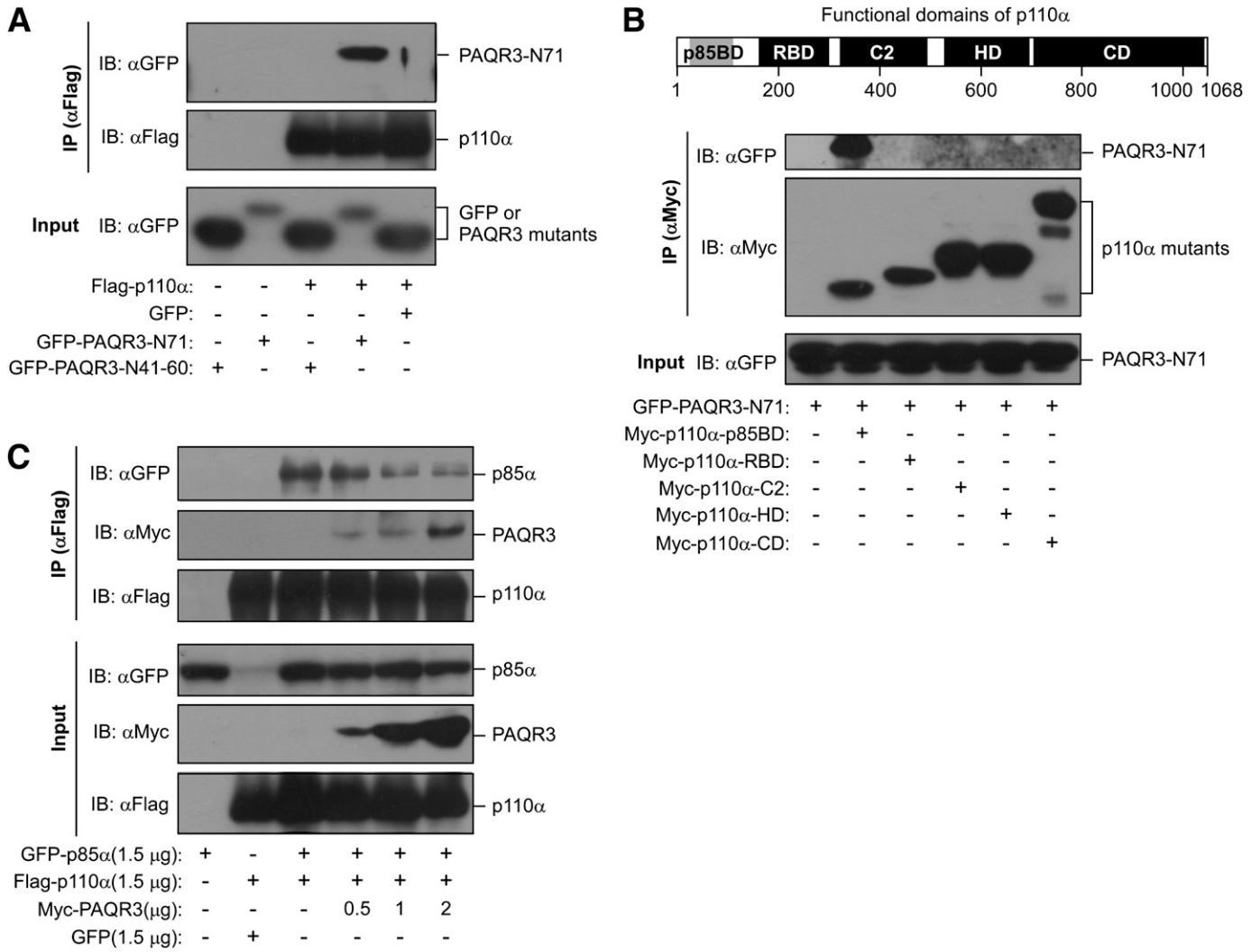

FIG. 8. PAQR3 reduces p85α binding with p110α. HEK293T cells were transiently transfected with the plasmids as indicated. The cell lysate was used in immunoblotting (IB) and immunoprecipitation (IP) using the antibodies as indicated. *A*: Interaction of the NH_2-terminal end of PAQR3 with p110α. Two PAQR3 mutants were used in the assay: PAQR3-N71 contained the NH_2-terminal 71 amino acid residues fused to GFP, and PAQR3-N41-60 contained 20 amino acid residues fused to GFP. *B*: Interaction of PAQR3-N71 with different functional domains of p110α. The functional domains of p110α are shown in *B* (*top*) as darkened boxes with the number of amino acid residues marked in the bottom. *C*: PAQR3 overexpression dose-dependently reduces the interaction between p110α and p85α, as measured by competition for coimmunoprecipitation.

and glucose tolerance test of the mice (at 12 weeks of age) were not significantly altered by *Paqr3* deletion (Fig. 9*D* and *E*). However, the insulin sensitivity, as determined by insulin tolerance test, was apparently elevated by *Paqr3* deletion (Fig. 9*F*), thus providing additional in vivo evidence that PAQR3 is implicated in the modulation of insulin signaling.

DISCUSSION

Subcellular compartmentalization is now recognized as a means to fine-tune intracellular signal transduction. For example, Ras proteins are spatially and temporally trafficked within cells, depending on the extracellular stimuli and cellular context (29). Compartmentalized signaling controls the intensity of signaling output and modulates cell function by altering the distribution and/or sequestration of signaling molecules. Specifically, distinct subcellular partitioning of endogenous subunits of PI3K has been reported. The p110β subunit localizes to the nucleus, and such localization is required for p110β to implement its effect on cell survival (30); similarly, Golgi-localized p110δ is crucial for its regulation of tumor necrosis factor trafficking and secretion (31). In contrast, the subcellular compartmentalization of the p110α subunit has proved elusive despite its principal role within the PI3K family in mediating insulin signaling (10–12).

In this study, we report a previously unrecognized mode of spatial regulation of p110α by PAQR3, a transmembrane protein specifically localized in the Golgi apparatus (17). Through its interaction with p110α, PAQR3 sequesters p110α to the Golgi apparatus, thereby reducing insulin-induced, p110α-mediated signaling. Based on immunostaining, under basal conditions, endogenous p110α was mainly localized in three areas: the cytosol, Golgi apparatus, and nucleus (Fig. 2*A*). It is reasonable to assume that only the cytosol-localized p110α is available to participate in IR-mediated PI3K signaling on the PM. Hence, we evaluated the relative partitioning of p110α between the Golgi and cytosol as an indication of the potential contribution of PAQR3-mediated Golgi compartmentalization of p110α to p110α-mediated signaling. We found that the presence or absence of PAQR3 can clearly change the balance between

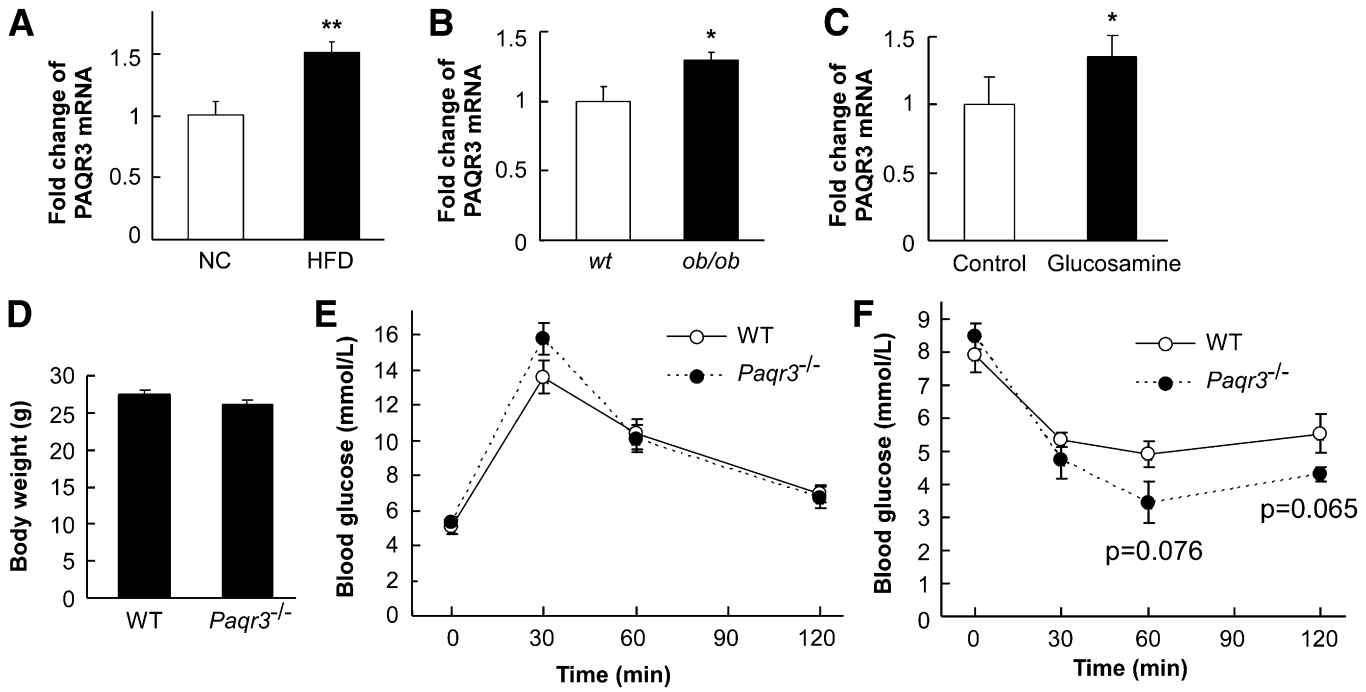

FIG. 9. PAQR3 expression is altered in insulin-resistant conditions, and *Paqr3* deletion increases insulin sensitivity. *A–C*: The mRNA level of PAQR3 was analyzed in the liver of mice fed with normal chow (NC) or HFD for 16 weeks (n = 7 for NC and n = 8 for HFD) (*A*), in the liver of wild-type and *ob/ob* mice (n = 6 for each group) (*B*), and in glucosamine-treated primary mouse hepatocytes (*C*). All data are shown as means ± SEM. *P < 0.05 and **P < 0.01 between the two groups. *D–F*: The effect of *Paqr3* deletion on body weight (*D*), glucose tolerance test (*E*), and insulin tolerance test (*F*). The mice were ~12 weeks of age at the time of the experiment (n = 8 for each group). All the data are shown as means ± SEM, and the P value from two-sided Student t test is indicated.

cytosolic and Golgi-localized p110α. Knockdown of PAQR3 in HEK293T cells increased cytosolic p110α (Fig. 2*A*). Concomitantly, the Golgi-localized p110α was reduced by PAQR3 knockdown (Fig. 2*A*). Using the data in HEK293T cells as a calculation reference, complete deletion of *Paqr3* would deplete all Golgi-localized p110α and result in a change of cytosolic p110α from 73 to 100%, leading to a 37% net increase in cytosolic p110α available for its signaling. Consistently, ablation of *Paqr3* leads to an ~20–50% increase in PIP3 production and PI3K activity (Fig. 3*B–D*), ~30–50% increase in insulin signaling, as judged by insulin-stimulated phosphorylation of AKT and GSK3β (Figs. 5 and 6), and ~30–40% elevation in insulin-stimulated GLUT4 translocation to the cell surface and glucose uptake (Fig. 7). Based on these data, we propose that PAQR3-mediated alteration in p110α compartmentalization may contribute to an ~30–50% change in insulin-stimulated PI3K activity in the liver and skeletal muscle.

In highlighting the important contribution of PAQR3 to p110α-mediated signaling, this immunolocalization was complemented by our biochemical analysis using purified, isolated Golgi fractions, where Golgi localization of endogenous p110α was abrogated by *Paqr3* ablation (Fig. 2*C*). Consistently, the relative distribution of p110α in the cytosolic and membranous fractions is altered by the expression level of PAQR3 (Fig. 2*D* and *E*). Most importantly, deletion of *Paqr3* leads to an increase in insulin-stimulated PI3K activity and PIP3 production in hepatocytes (Fig. 3*B–D*). On the other hand, overexpression of PAQR3 reduces insulin-stimulated PI3K activity and PIP3 production (Fig. 3*E* and *F*). Collectively, these data provide compelling evidence that PAQR3 is able to regulate the compartmentalization and activity of p110α.

Experiments aimed at mapping the domains involved in the interaction between PAQR3 and p110α reveal that the p85 binding domain of p110α mediates the interaction of p110α with PAQR3 (Fig. 8*B*). Furthermore, overexpression of PAQR3 could dose-dependently reduce the interaction of p110α with p85 (Fig. 8*C*). These data, therefore, indicate that PAQR3 negatively modulates PI3K activity by preventing p85 from forming a complex with p110α while sequestering p110α to the Golgi apparatus. Based on these data, we propose that p110α-mediated insulin signaling is modulated by the intracellular availability of PAQR3. Cells with a high expression level of PAQR3 would sequester a greater proportion of p110α in the Golgi apparatus, thereby decreasing the cytosolic portion of p110α available to relay the signaling from the IR to downstream effectors, and leading to a reduction in insulin action. In agreement with this idea, our data indicate that the expression level of PAQR3 is correlated with the development of insulin resistance. The mRNA level of *Paqr3* was elevated in the livers of both HFD and *ob/ob* mice as well as in glucosamine-induced insulin-resistant hepatocytes (Fig. 9*A–C*). Consistently, deletion of *Paqr3* could increase insulin sensitivity in vivo (Fig. 9*F*). These findings, therefore, indicate that changes of PAQR3 expression may represent a new mechanism underlying the compromised PI3K activity under pathophysiological conditions. It has previously been demonstrated that IRS-associated PI3K activity is decreased significantly in *ob/ob* mouse liver (32) and that AKT activity is reduced in the liver and skeletal muscle in diabetic rats (33). It will be intriguing to determine in the future whether the comprised PI3K activity observed in these studies as well as in human diabetic patients is caused by alterations of PAQR3 expression.

Considering the importance of PAQR3 in modulating PI3K activity, it will be crucial to identify the factors or conditions involved in regulating PAQR3 transcription and/or availability. Finally, modulating the expression of PAQR3 or its interaction with p110α may comprise a new strategy to control PI3K activity to combat insulin resistance.

ACKNOWLEDGMENTS

This work was supported by research grants from the Ministry of Science and Technology of China (2012CB524900 to Y.C. and 2010CB529506 to Y.P. and Z.W.), the National Natural Science Foundation of China (30830037, 81021002, and 81130077 to Y.C. and 30971660 to Y.P.), and the Chinese Academy of Sciences (KSCX2-EW-R-08 to Y.C.).

No potential conflicts of interest relevant to this article were reported.

X.W. and L.W. conceived, designed, and performed the experiments; analyzed data; and wrote the manuscript. L.Z., F.X., and W.L. performed the experiments. Y.P., Z.W., F.G., Y.L., and W.G.T. contributed the reagents, material and analysis tools, and editorial assistance. Y.C. conceived and designed the experiments, analyzed data, and wrote the manuscript. Y.C. is the guarantor of this work and, as such, had full access to all the data in the study and takes responsibility for the integrity of the data and the accuracy of the data analysis.

The authors thank Dr. Joachim Seemann (University of Texas Southwestern Medical Center, Dallas, TX) for providing the protocol for Golgi isolation of mouse liver.

REFERENCES

1. Kahn SE, Hull RL, Utzschneider KM. Mechanisms linking obesity to insulin resistance and type 2 diabetes. Nature 2006;444:840–846
2. Fruman DA, Meyers RE, Cantley LC. Phosphoinositide kinases. Annu Rev Biochem 1998;67:481–507
3. Vanhaesebroeck B, Guillermet-Guibert J, Graupera M, Bilanges B. The emerging mechanisms of isoform-specific PI3K signalling. Nat Rev Mol Cell Biol 2010;11:329–341
4. Engelman JA, Luo J, Cantley LC. The evolution of phosphatidylinositol 3-kinases as regulators of growth and metabolism. Nat Rev Genet 2006;7:606–619
5. Taniguchi CM, Kondo T, Sajan M, et al. Divergent regulation of hepatic glucose and lipid metabolism by phosphoinositide 3-kinase via Akt and PKClambda/zeta. Cell Metab 2006;3:343–353
6. Okkenhaug K, Bilancio A, Farjot G, et al. Impaired B and T cell antigen receptor signaling in p110delta PI 3-kinase mutant mice. Science 2002;297:1031–1034
7. Clayton E, Bardi G, Bell SE, et al. A crucial role for the p110delta subunit of phosphatidylinositol 3-kinase in B cell development and activation. J Exp Med 2002;196:753–763
8. Bi L, Okabe I, Bernard DJ, Wynshaw-Boris A, Nussbaum RL. Proliferative defect and embryonic lethality in mice homozygous for a deletion in the p110alpha subunit of phosphoinositide 3-kinase. J Biol Chem 1999;274:10963–10968
9. Bi L, Okabe I, Bernard DJ, Nussbaum RL. Early embryonic lethality in mice deficient in the p110beta catalytic subunit of PI 3-kinase. Mamm Genome 2002;13:169–172
10. Foukas LC, Claret M, Pearce W, et al. Critical role for the p110alpha phosphoinositide-3-OH kinase in growth and metabolic regulation. Nature 2006;441:366–370
11. Sopasakis VR, Liu P, Suzuki R, et al. Specific roles of the p110alpha isoform of phosphatidylinsositol 3-kinase in hepatic insulin signaling and metabolic regulation. Cell Metab 2010;11:220–230
12. Knight ZA, Gonzalez B, Feldman ME, et al. A pharmacological map of the PI3-K family defines a role for p110alpha in insulin signaling. Cell 2006;125:733–747
13. Jia S, Liu Z, Zhang S, et al. Essential roles of PI(3)K-p110beta in cell growth, metabolism and tumorigenesis. Nature 2008;454:776–779
14. Yamauchi T, Kamon J, Ito Y, et al. Cloning of adiponectin receptors that mediate antidiabetic metabolic effects. Nature 2003;423:762–769
15. Bjursell M, Ahnmark A, Bohlooly-Y M, et al. Opposing effects of adiponectin receptors 1 and 2 on energy metabolism. Diabetes 2007;56:583–593
16. Tang YT, Hu T, Arterburn M, et al. PAQR proteins: a novel membrane receptor family defined by an ancient 7-transmembrane pass motif. J Mol Evol 2005;61:372–380
17. Feng L, Xie X, Ding Q, et al. Spatial regulation of Raf kinase signaling by RKTG. Proc Natl Acad Sci USA 2007;104:14348–14353
18. Luo X, Feng L, Jiang X, et al. Characterization of the topology and functional domains of RKTG. Biochem J 2008;414:399–406
19. Xie X, Zhang Y, Jiang Y, et al. Suppressive function of RKTG on chemical carcinogen-induced skin carcinogenesis in mouse. Carcinogenesis 2008;29:1632–1638
20. Fan F, Feng L, He J, et al. RKTG sequesters B-Raf to the Golgi apparatus and inhibits the proliferation and tumorigenicity of human malignant melanoma cells. Carcinogenesis 2008;29:1157–1163
21. Zhang Y, Jiang X, Qin X, et al. RKTG inhibits angiogenesis by suppressing MAPK-mediated autocrine VEGF signaling and is downregulated in clear-cell renal cell carcinoma. Oncogene 2010;29:5404–5415
22. Jiang Y, Xie X, Zhang Y, et al. Regulation of G-protein signaling by RKTG via sequestration of the G betagamma subunit to the Golgi apparatus. Mol Cell Biol 2010;30:78–90
23. Bartz R, Sun LP, Bisel B, Wei JH, Seemann J. Spatial separation of Golgi and ER during mitosis protects SREBP from unregulated activation. EMBO J 2008;27:948–955
24. Wei JH, Seemann J. The mitotic spindle mediates inheritance of the Golgi ribbon structure. J Cell Biol 2009;184:391–397
25. Gray A, Olsson H, Batty IH, Priganica L, Peter Downes C. Nonradioactive methods for the assay of phosphoinositide 3-kinases and phosphoinositide phosphatases and selective detection of signaling lipids in cell and tissue extracts. Anal Biochem 2003;313:234–245
26. Várnai P, Bondeva T, Tamás P, et al. Selective cellular effects of overexpressed pleckstrin-homology domains that recognize PtdIns(3,4,5)P3 suggest their interaction with protein binding partners. J Cell Sci 2005;118:4879–4888
27. Park WS, Heo WD, Whalen JH, et al. Comprehensive identification of PIP3-regulated PH domains from *C. elegans* to *H. sapiens* by model prediction and live imaging. Mol Cell 2008;30:381–392
28. Taniguchi CM, Emanuelli B, Kahn CR. Critical nodes in signalling pathways: insights into insulin action. Nat Rev Mol Cell Biol 2006;7:85–96
29. Harding A, Tian T, Westbury E, Frische E, Hancock JF. Subcellular localization determines MAP kinase signal output. Curr Biol 2005;15:869–873
30. Kumar A, Redondo-Muñoz J, Perez-García V, Cortes I, Chagoyen M, Carrera AC. Nuclear but not cytosolic phosphoinositide 3-kinase beta has an essential function in cell survival. Mol Cell Biol 2011;31:2122–2133
31. Low PC, Misaki R, Schroder K, et al. Phosphoinositide 3-kinase δ regulates membrane fission of Golgi carriers for selective cytokine secretion. J Cell Biol 2010;190:1053–1065
32. Nawano M, Ueta K, Oku A, et al. Hyperglycemia impairs the insulin signaling step between PI 3-kinase and Akt/PKB activations in ZDF rat liver. Biochem Biophys Res Commun 1999;266:252–256
33. Kerouz NJ, Hörsch D, Pons S, Kahn CR. Differential regulation of insulin receptor substrates-1 and -2 (IRS-1 and IRS-2) and phosphatidylinositol 3-kinase isoforms in liver and muscle of the obese diabetic (*ob/ob*) mouse. J Clin Invest 1997;100:3164–3172